Chemical Engineering Journal 435 (2022) 135078

Contents lists available at ScienceDirect

Chemical Engineering Journal

journal homepage: www.elsevier.com/locate/cej

Adsorption or direct interspecies electron transfer? A comprehensive investigation of the role of biochar in anaerobic digestion of hydrothermal liquefaction aqueous phase

Zixin Wang [a], Cheng Zhang [b], Jamison Watson [a], Brajendra K. Sharma [c,d], Buchun Si [e,*], Yuanhui Zhang [a,*]

[a] Department of Agricultural and Biological Engineering, University of Illinois at Urbana-Champaign, Urbana, IL 61801, USA
[b] Department of Chemical and Biomolecular Engineering, University of Illinois at Urbana-Champaign, Urbana, IL 61801, USA
[c] Prairie Research Institute—Illinois Sustainable Technology Center, University of Illinois at Urbana-Champaign, Urbana, IL 61820, USA
[d] United States Department of Agriculture, Agricultural Research Service Eastern Regional Research Center, Wyndmoor, PA 19038-8598, USA
[e] Laboratory of Environment-Enhancing Energy (E2E), Key Laboratory of Agricultural Engineering in Structure and Environment, Ministry of Agriculture, College of Water Resources and Civil Engineering, China Agricultural University, Beijing 100083, China

ARTICLE INFO

Keywords:
Anaerobic digestion
Biochar
Hydrothermal liquefaction aqueous phase
Adsorption
Microbial community
Direct interspecies electron transfer

ABSTRACT

Hydrothermal liquefaction (HTL) is promising for the conversion of biowaste into biofuels, but the energy recovery from the HTL aqueous phase (HTL-AP) by anaerobic digestion is limited due to its degradability resistance. Adding biochar was reported to facilitate digestion, but its role has not been explicitly determined. Direct interspecies electron transfer (DIET) was reported to participate and dominate the digestion process; however, the adsorption and detoxification effects of biochar cannot be ignored. This study is conducted to confirm the exact role of biochar and its primary mechanism on the digestion process. Results showed that the total pore volume and adsorption capacity of biochar played the most influential role. In comparison, DIET was very likely not dominant due to the limited electrical conductivity and electron-donating/accepting capacities of biochar. The microbial analysis further indicated that mediated interspecies electron transfer remained the primary mechanism rather than DIET. The addition of facilitative biochar promoted the enrichment of *Thermovirga* and *Methanosaeta*, whereas a suppressive biochar addition shifted the dominant microbes to *Asaccharospora, Clostridium,* and *Methanobacterium*. Furthermore, a Random Forest prediction model was developed, with an accuracy of 87%, to forecast whether DIET dominantly influenced methane generation with biochar addition. This study proved that the effect of biochar on anaerobic digestion of HTL-AP relied mainly on adsorption, mediated interspecies electron transfer was more effectively enhanced rather than DIET, and a modeling approach was developed to verify the presence of DIET.

1. Introduction

Global development has brought about extensive and continuous utilization of fossil fuels and has contributed to increasing greenhouse gas emissions. The formation of renewable energy systems is a global imperative to achieve sustainable development, and hydrothermal liquefaction (HTL) is a promising technology to realize sustainability. HTL is a thermochemical process that converts biowaste into biofuels, which could be further upgraded into transportation fuels. Mobile, pilot-scale HTL has been achieved and the upgraded oil is chemically, physically, and thermally similar to gasoline, diesel, and Jet A fuel [1,2]. However, utilization of the HTL aqueous phase (HTL-AP) was restricted. HTL-AP is a high nutrient content product. Its average chemical oxygen demand (COD) value could be as high as 81.9 g/L [3]. Anaerobic digestion is a commonly used method to recover these nutrients and energy, but the degradation efficiency is low with 33–64% of organics remaining in the anaerobic slurry after digestion [4].

Adding biochar, a carbonaceous product from the thermochemical treatment of biomass has proven to be an effective method to enhance digestion efficiency [5–7]. With a large surface area, porous structure, great ion exchange capacity, stable structure, and abundance of functional groups, biochar brings several benefits to the digestion process

* Corresponding authors.
E-mail addresses: sibuchun@cau.edu.cn (B. Si), yzhang1@illinois.edu (Y. Zhang).

https://doi.org/10.1016/j.cej.2022.135078
Received 22 November 2021; Received in revised form 10 January 2022; Accepted 1 February 2022
Available online 4 February 2022
1385-8947/© 2022 Elsevier B.V. All rights reserved.

[8]. First, biochar can function as an adsorbent to sequester toxic inhibitory substances and alleviate their inhibition to anaerobic microbes. Second, the large surface area and porous structure provide more sites for microbial colonization and enhance their interactions. Third, the alkaline nature makes biochar a pH buffer to stabilize the digestion process, especially for the acidic substrates.

Moreover, recent studies reported that biochar addition could stimulate the establishment of direct interspecies electron transfer (DIET) during anaerobic digestion [9–12]. DIET has been proposed to have a higher efficiency and more stable transfer of reducing equivalents between electron-donating bacteria and electron-accepting archaea than traditional mediated hydrogen/formate interspecies electron transfer [13–15]. DIET could be assisted by biological connections with nanowires and cytochromes as well as by adding conductive materials [16], such as biochar. For example, Wang et al. found that the electron exchange capacity of biochar contributed to the DIET process, which shortened the lag time and improved the methane production rate [9]. Ren et al. also reported that hydrochar from HTL could induce DIET through its surface oxygen-containing functional groups and facilitate a more efficient digestion performance [17].

In contrast to the extensively investigated adsorption and detoxification capacity, direct evidence for the occurrence of biochar-induced DIET is lacking in most studies. The claims about the potential role of biochar also varied. Qi et al. found enhanced conductivity of biochar with a graphene structure, and the improved bioavailability of trace elements was related to DIET [10]. Nevertheless, Viggi et al. reported that the electron-donating capacity of biochar affected DIET and methanogenesis, while other key factors including electrical conductivities, specific surface areas, and electron-accepting capacities only had limited effects [18]. The establishment of DIET has also been questioned. Lü et al. stated that biochar could be involved in methanogenesis as a reducing equivalent, but DIET was not set up due to the low conductivity [19]. These different results suggest that the role of biochar in anaerobic digestion needs further clarification.

In this study, nine physical and chemical properties of five types of biochar were evaluated, adsorption experiments were performed to investigate the adsorption kinetics of biochar, and the relationship between biochar addition, microbial structure, and metabolism were investigated to verify the role of biochar in organic conversion and methane generation. In addition, a Random Forest model was developed to predict the presence of DIET with biochar. Information obtained here would contribute to a better understanding of the function and influence of biochar addition and provide a reference for the verification of DIET establishment.

2. Materials and methods

2.1. Sample preparation

Biochar samples were produced from different biomass sources under different reaction conditions [20]. Biochar-B, biochar-C, biochar-D, and biochar-F were converted from the slow pyrolysis of corn stalks, switchgrass, hardwood, and *Miscanthus* at 450 °C, respectively. Biochar-E was produced from the gasification of corn stalk at 800–900 °C. Commercial Calgon F-400 granular activated carbon (GAC) was prepared as a positive control.

The HTL-AP for anaerobic digestion was collected after a pilot-scale HTL experiment of swine manure which was conducted at 270 ± 10 °C with a retention time of 1 h. The HTL-AP was stored at room temperature and filtered by a 0.45 μm filter before use.

The inoculum was collected after anaerobic digestion in the Champaign & Urbana Sanitary District (Urbana, Illinois, USA) and cultivated by synthetic wastewater (1 g COD/L) as previously reported [4]. Then, the inoculum was washed 3 times with DI water and centrifuged at 3000 rpm for 10 min before use.

2.2. Experimental setup

Batch tests were performed in 7 groups in triplicate (GAC, biochar-B, biochar-C, biochar-D, biochar-E, biochar-F, and control). Serum bottles with a working volume of 160 mL were used, and 30 mL inoculum was added. The initial substrate concentration was 10 g COD/L. Biochar and GAC samples were added with a concentration of 10 g/L. Anaerobic digestion was operated at 37 ℃ using a water bath for 29 days. The gas volume and gas content were measured daily with a glass syringe and gas chromatography (Shimadzu GC-780), respectively.

The adsorption experiments were conducted using phenol, pyridine, and hydroxypyridine with a concentration of 100 mg/L. The concentrations of biochar and GAC were 10 g/L. The experiments were conducted at 37 ℃ with a pH of 6.5 (to be consistent with anaerobic digestion conditions) for 48 h.

2.3. Analytical methods

The Brunauer Emmett Teller (BET) specific surface area and Barrett Joyner Halenda (BJH) pore volume of biochar and GAC were measured via N_2 adsorption at 77 K using a Micromeritics 3Flex system. Elemental analysis was conducted with a CE440 element analyzer, and the oxygen content was calculated by difference. Surface functional groups of biochar were measured via Fourier transform infrared spectroscopy (FTIR) using a Thermo Nicolet Nexus 670 spectrophotometer.

The electron-donating and electron-accepting capacities were calculated with mediated electrochemical reduction (MER) and oxidation (MEO) according to a previously reported method [21]. Electron transfer mediators DQ (in MER) or ABTS (in MEO) were added and resulted in reductive and oxidative current peaks after the working electrode equilibrated to the desired redox potential (−0.69 V for MER and 0.61 V for MEO). Then, the current peaks were integrated to get the electron transfer capacities:

$$\text{Electron}-\text{accepting capacity} = \frac{\int \frac{I_{red}}{F} dt}{m_{biochar}},\ \text{electron}-\text{donating capacity} = \frac{\int \frac{I_{ox}}{F} dt}{m_{biochar}}$$

where I_{red} and I_{ox} (A) are the reductive and oxidative currents in MEO and MER, respectively, $F = 96{,}485$ s A/mol$_{e^-}$ is the Faraday constant, and $m_{biochar}$ (g) is the mass of biochar and GAC.

Electrical conductivity was calculated from the electrical resistance with the voltammetric response according to a previously reported method [18]. The biochar or GAC powder was pressed between two cylindrical steel pistons with a diameter of 20 mm to form a pellet. The resistance of the obtained pellet was measured by recording the current response when applying potential: $V = R \bullet I$, where V is the potential (V), R is the electrical resistance (Ω), and I is the current (A). Then, the electrical conductivity was calculated using the following equation: $\sigma = \frac{l}{R \bullet S}$, where σ is the electrical conductivity (S/m), l is the thickness of the pellet (m), and S is the area of the cross-section of the pellet (m^2).

A pseudo-first-order adsorption kinetic model was used to fit the adsorption curve of phenol, pyridine, and hydroxypyridine:

$$ln\left(q_{eq} - q_t\right) = lnq_{eq} - kt$$

where q_{eq} and q_t are the adsorption capacity (mg/g) at equilibrium and at time t (hour), respectively, and k (hr^{-1}) is the adsorption rate constant.

A modified Gompertz model was used to fit the methane production curve:

$$M = P_{max} \bullet \exp\left\{-\exp\left[\left(\frac{R_{max} \bullet e}{P_{max}}\right) \bullet (\lambda - t) + 1\right]\right\}$$

where M is the accumulated methane yield at time t (mL/g COD), P_{max} is

the maximum methane yield potential (mL/g COD), R_{max} is the maximum methane production rate (mL/(g • d) COD), λ is the lag phase (d), and t is the fermentation time (d).

A Random Forest model was used to predict the presence of DIET concerning the biochar properties. Missing values were imputed by missForest before making model predictions. The model was built with set.seed (701).

Chemical oxygen demand (COD) was measured by a Hach spectrophotometer (Model DR3900). High-performance liquid chromatography (HPLC) (Shimadzu Scientific Instruments) equipped with an Aminex HPX-87H column (Bio-Rad) was used to measure the concentration of volatile fatty acids (VFAs). The mobile phase was 5 mM H_2SO_4 and the column temperature was 40 ℃. The concentration of phenol, pyridine, and hydroxypyridine was measured by HPLC at 254 nm at room temperature with a C_{18} reverse-phase column. The mobile phase consisted of methanol:water (4:1 v/v). The organic composition was measured by GC–MS and analyzed with the Mass Spectral Database (NIST08). The anaerobic effluent was also measured by MALDI-TOF-MS with a Brucker Auto-Flex Speed MALDI system.

The microbial structure was characterized by Illumina Miseq sequencing according to a previously reported method [22].

3. Results and discussion

3.1. Effects of biochar addition on methane production

Methane production was fitted with a modified Gompertz model (Fig. 1). The maximum methane yield (186.5 ± 3.4 mL CH_4/g COD) was observed with GAC addition followed by biochar-E (185.2 ± 1.2 mL CH_4/g COD), which were 10.4% and 9.6% higher than the control (169.0 ± 2.4 mL CH_4/g COD), respectively (Table 1). The optimal promotion by biochar was as good as GAC, indicating the potential of biochar to promote methanogenesis. Considering the methane production rate, biochar-E facilitated the maximum increase of 16.2% among all the biochar groups, while GAC addition promoted a 34.2% higher production rate than the control. The lag phase could also be shortened with biochar inclusion, amounting to an optimal 15.3% reduction in the biochar-C group. GAC showed superior performance over biochar in both methane production and system stability, suggesting that GAC and biochar may not always function in the same way during anaerobic digestion [23,24]. It is also worth noting that the effect of biochar addition varied, resulting in biochar-D addition inhibiting both methane generation and lag phase reduction. An 11.1% lower yield and a 14.7% longer lag phase were observed in the biochar-D group. The different reaction performances could be attributed to the different properties of the added materials. Physical and chemical characteristics of the

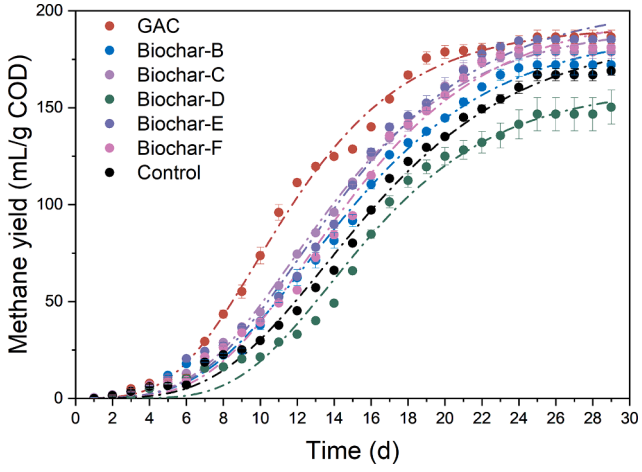

Fig. 1. Methane production with biochar addition.

Table 1
Parameters of modified Gompertz model.

Group	M_m (mL CH_4/g COD)	R_m (mL CH_4/g COD/d)	λ(d)	R^2
GAC	186.5 (3.4)	15.7 (0.7)	5.33 (0.2)	0.996
Biochar-B	172.1 (5.3)	12.1 (0.7)	6.78 (0.4)	0.995
Biochar-C	178.8 (3.3)	13.5 (0.6)	6.47 (0.2)	0.997
Biochar-D	150.3 (8.8)	11.7 (1.1)	8.76 (0.5)	0.988
Biochar-E	185.2 (1.2)	13.6 (0.8)	6.77 (0.4)	0.994
Biochar-F	181.2 (1.2)	13.4 (0.9)	7.16 (0.4)	0.993
Control	169.0 (2.4)	11.7 (0.7)	7.64 (0.4)	0.995

different biochars influence their interactions with microbial communities and determine the organic conversion efficiency during digestion. Detailed analysis will be provided in the following sections.

3.2. Relationship between biochar properties and their roles in methane production

Surface area, total pore volume, electrical conductivity, and the electron-accepting/donating capacities of biochar were measured (Table 2). The surface areas of all biochar in this study were low, with the largest being 48.4 m^2/g in the biochar-E group. The low surface area makes it difficult to harbor enough important microbes for methane production, and it may also lead to a lower aggregation extent of biochar and microbes, which is important for electron transfer [25]. As for the total pore volume (see Fig. A.1 for the pore morphology of biochar), biochar-D had a 34.6–105.9% larger value than other samples. During the start-up period of digestion, substances attach to the biochar surface and form a core that facilitates rapid microbial aggregation [12]. A pore volume that is too large may be detrimental to this granulation process, which could be one reason for the poor gas production performance of biochar-D. Meanwhile, a pore volume that is too small may also be unfavorable for such aggregation and might be partially responsible for the low methane yield of biochar-B. No significant differences were observed between biochar groups concerning the electron-accepting and donating capacities, suggesting that the differences in methane generation were not related to the electrochemical properties of the added biochar. Compared to biochar, GAC had a 17.2–84.3 times larger surface area, a 4.5–9.2 times larger total pore volume, and the electrical conductivity and electron-donating/accepting capacities were much better than biochar. These characteristic differences indicated that the addition of GAC and biochar may have different roles in anaerobic digestion.

Previous studies proposed that the electrochemical properties, such as conductivity and redox activity, enable biochar to act as an electron conduit between electron-donating bacteria and electron-accepting archaea. Electron transfer can take place through redox cycling via redox-active surface groups and through direct transfer via the carbon matrices in biochar [21,25,26]. However, the electrical conductivities of the biochar (Table 2) were relatively low in this study, and the electron-donating capacities and electron-accepting capacities remained at low levels. The low values could be related to the biochar production process and suggest that DIET may not play an important role in promoting digestion. In addition, previous studies also reported that the sludge conductivity can be enhanced after digestion because the establishment of DIET-induced enrichment of pili accounted for the increased conductivity. The increase in sludge conductivity was set as evidence for the presence of DIET, which can be 1.6–82.0 times higher compared to the inoculum or control [16]. However, sludge conductivities in all biochar-assisted reactors were very low (almost non-conductive) in this study (Table 3), indicating that mediated interspecies electron transfer still dominated the reactions.

Elemental analysis (Table 2) can further help compare the different properties of biochar and reveal their role in anaerobic digestion. Compared with other biochar groups, biochar-E had the lowest hydrogen to carbon (H/C) ratio, indicating a higher degree of

Table 2
Physical and chemical properties of biochar.

Properties	GAC	Biochar-B	Biochar-C	Biochar-D	Biochar-E	Biochar-F
Surface area (m^2/g)	834.4	9.9	11.3	28.5	48.4	18.5
Total pore volume (cm^3/g)	0.157	0.017	0.018	0.035	0.022	0.026
Electrical conductivity (S/m)	3.49E−02	1.56E−09	1.13E−09	3.29E−09	1.07E−04	2.03E−09
Electron donating capacity (meq/g)	2.32E−05	6.08E−07	1.79E−07	6.17E−07	3.51E−07	8.10E−07
Electron accepting capacity (meq/g)	1.11E−03	6.66E−06	4.50E−05	2.88E−05	2.42E−05	6.84E−06
C (wt%)	82.66	68.27	72.64	78.91	64.20	74.80
H (wt%)	0.71	2.97	3.42	3.24	2.07	3.19
N (wt%)	0.59	1.21	1.24	0.91	1.31	0.80
O (wt%)*	16.04	27.55	22.70	16.94	32.42	21.21
H/C ratio	0.01	0.04	0.05	0.04	0.03	0.04
O/C ratio	0.19	0.40	0.31	0.21	0.50	0.28

Table 3
Sludge conductivities with biochar addition.

Sludge conductivity (S/m)	GAC	Biochar-B	Biochar -C	Biochar -D	Biochar -E	Biochar -F	Control
	4.32E−11 (7.95E−12)	8.03E−11 (1.91E−11)	2.79E−11 (1.57E−12)	1.03E−10 (1.03E−11)	3.83E−10 (4.14E−11)	1.32E−10 (4.80E−11)	6.04E−11 (1.74E−11)

unsaturation that could be related to the stronger adsorption capacity [27]. H/C ratio can be negatively correlated with surface area and positively correlated with the mobile matter content (the organic portion of biochar), which is consistent in biochar-E [28]. Moreover, Wei et al. (2020) found that the adsorption of biochar was dominated by pore-filling when the H/C ratio was below 0.5, while adsorption was dominated by the surface chemical bond when it was above 0.5 [28]. Since the H/C ratio of all groups was less than 0.5, pore-filling-related parameters, such as surface area and pore volume, are therefore important in determining the adsorption capacity.

Biochar-E also had the highest oxygen to carbon (O/C) ratio, which can be an indicator of the abundance of oxygen-containing functional groups. FTIR results showed that oxygen-containing functional groups, including C-O, C═O, and C-OH, were abundant in biochar, and the C═O and C-O functional groups were significantly more abundant than GAC (Fig. 2). The presence of oxygen-containing functional groups correlated with the methane generation efficiency, where the related quinone and hydroquinone moieties could make biochar redox-active and participate in electron transfer between microbes [17]. However, the possibility for biochar to serve as electron conduits participating in electron transfer is relatively low because of its low electron-accepting/donating capacity.

The adsorption capacity of biochar was considerable and could play

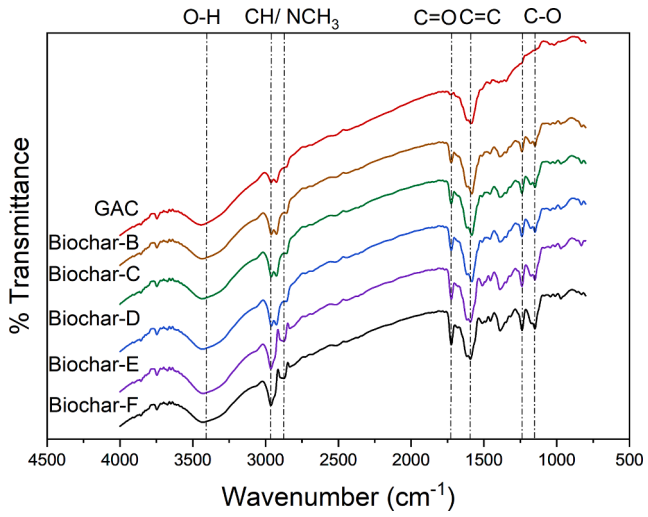

Fig. 2. Functional groups of biochar.

an important role in digestion [29]. Adsorption experiments of phenol, pyridine, and hydroxypyridine, which are three representative inhibitory chemicals in HTL-AP, were performed, and a pseudo-first-order kinetic model was used to fit the adsorption process (Fig. 3, Table 4). Results showed that the model fitted the adsorption of phenol and hydroxypyridine well, and the fitted equilibrium adsorption capacities (q_{eq}) were consistent with the experimental value of 10 mg/g. Biochar-E and biochar-F had higher adsorption rates, with 1.6–2.0 and 3.8–4.4 times higher rate constants than those of biochar-D for phenol and hydroxypyridine, respectively. The adsorption of pyridine was not very compatible with first-order kinetics, indicating it could be second or greater order, but it was still evident that biochar-E and biochar-F had better adsorption capacities than others. These results were consistent with the fact that biochar-E and biochar-F promoted the highest methane production rate and yield. Biochar-C was also effective and was particularly good at adsorbing phenol. On the other hand, biochar-D showed the worst adsorption effects for all three compounds, so the toxic concentration in digesters with biochar-D remained high, and their inhibition on microorganisms could not be relieved. With a more complex composition of HTL-AP, the type of inhibitors can be more diverse, and the adsorption process of biochar can be more complex. However, these results provided a good perspective that the intrinsic properties of biochar affected their adsorption capacity, further influenced the environment for microbial growth, and altered system stability, which ultimately affected methane generation [7].

3.3. *Effects of biochar addition on organic degradation*

The COD removal efficiency was measured concerning biochar addition (Table A.1). Results showed that biochar-F facilitated the best COD removal of 74.5%, which was 8.7% higher than that of the control. Biochar-E, biochar-C, and biochar-B also showed promotion effects on chemical removal and exhibited comparable results (71.9–73.7%). However, biochar-D addition did not work as well as expected, resulting in 2.9% fewer chemicals being removed compared with the control, which was also consistent with its reduction in methane generation. Compared to biochar, the COD removal efficiency of GAC remained significant with 95.8% of the chemicals being removed, and it was 28.6% higher than biochar-F. These differences in COD removal were consistent with both the adsorption capacity of biochar and the differences in methane generation from organic compounds.

Conversion of VFAs was also monitored during anaerobic digestion. Results (Fig. 4) showed that biochar-E had the best removal effect

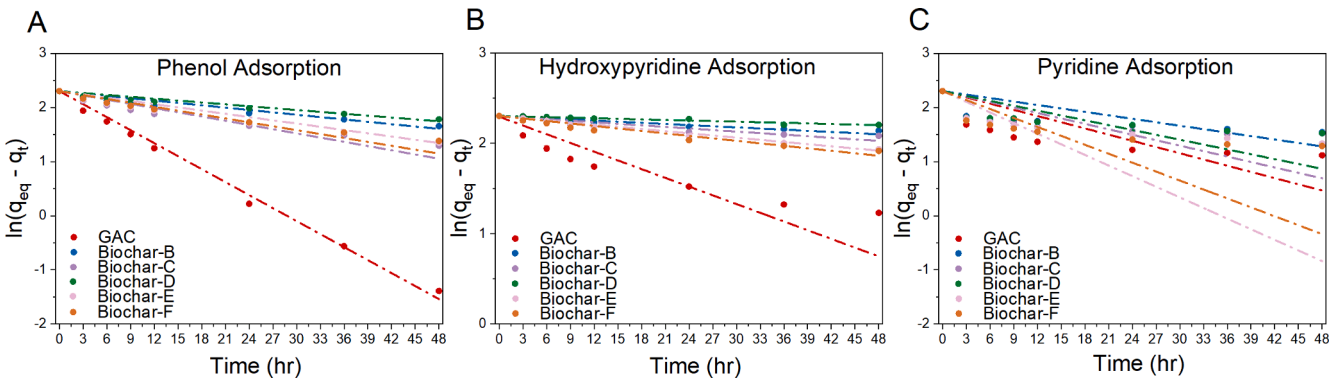

Fig. 3. Pseudo-first-order kinetic model for the adsorption of phenol (A), hydroxypyridine (B), and pyridine (C) by biochar (adsorption of pyridine was not very compatible with first-order kinetics, indicating it could be second or greater order. The figure here is intended to give a visual demonstration of the adsorption capacities of each biochar).

Table 4
Parameters of the pseudo-first-order adsorption kinetic models.

	Phenol			Hydroxypyridine			Pyridine		
	$k(hr^{-1})$	q_{eq} (mg/g)	R^2	$k(hr^{-1})$	q_{eq} (mg/g)	R^2	$k(hr^{-1})$	q_{eq} (mg/g)	R^2
GAC	8.0E−2 (2.3E−3)	10.0 (1.4E−4)	0.994	3.2E−2 (1.1E−3)	9.9 (2.6E−1)	0.992	3.8E−2 (9.5E−3)	10.0 (1.4E−3)	0.685
B	1.5E−2 (1.2E−3)	10.0 (2.4E−4)	0.955	4.2E−3 (2.9E−4)	10.0 (2.4E−2)	0.968	2.1E−2 (8.6E−3)	10.0 (7.4E−4)	0.420
C	2.6E−2 (1.1E−3)	10.0 (2.3E−4)	0.988	5.7E−3 (6.1E−4)	10.0 (2.9E−2)	0.925	3.4E−2 (5.8E−3)	10.0 (3.7E−4)	0.823
D	1.2E−2 (5.1E−4)	10.0 (1.3E−4)	0.987	2.1E−3 (1.8E−4)	10.0 (9.5E−3)	0.953	3.0E−2 (6.5E−3)	10.0 (8.5E−4)	0.739
E	2.0E−2 (3.1E−4)	10.0 (6.5E−4)	0.998	8.0E−3 (2.0E−4)	10.0 (1.7E−2)	0.996	6.5E−2 (1.9E−2)	10.0 (5.4E−4)	0.603
F	2.4E−2 (5.1E−4)	10.0 (1.9E−4)	0.997	9.2E−3 (4.3E−4)	10.0 (2.7E−2)	0.985	5.5E−2 (9.4E−3)	10.0 (5.3E−4)	0.828

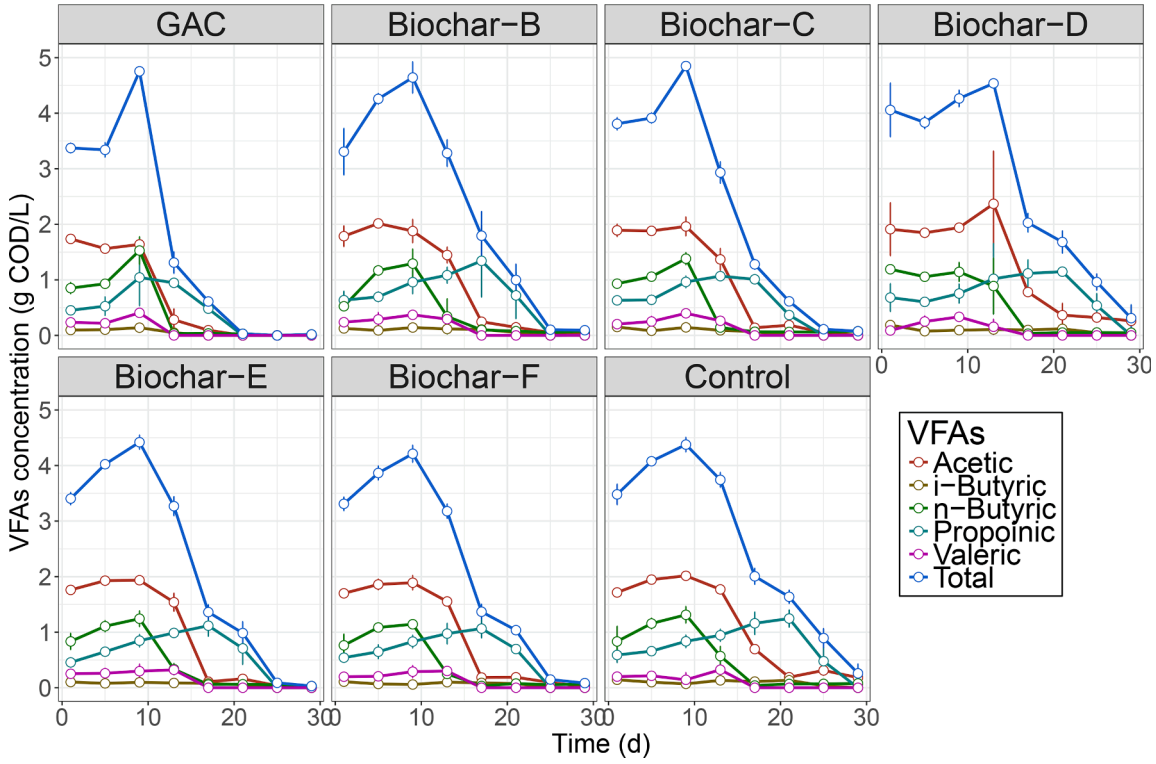

Fig. 4. Changes in VFAs with different biochar addition.

among the biochar groups, and the final concentration of total VFAs was less than 0.03 g COD/L, while the concentrations for biochar-D and the control were still high with values of 0.31 g COD/L and 0.26 g COD/L, respectively. It's also worth noting that the peak of organic acid accumulation occurred 4 days later for biochar-D than other groups, which was consistent with the longer lag phase (Fig. 2, Table 2). This result further proves that biochar-D was not good at releasing inhibition and improving system stability, especially during the early stage of digestion. Compared to biochar, a better degradation efficiency was observed in the GAC-amended reactor in which almost all VFAs were decomposed

after the 20th day. After 25 days, most of the VFAs were degraded in biochar-B, C, E, and F groups, but their concentration in biochar-D and the control reactors remained high. Specifically, the consumption of propionic acid exhibited an 8-day delay compared with other VFAs, and its concentration with biochar-D was still 1.15 g COD/L on the 21st day, which was 1.6–3.1 times higher than those with other biochar samples. Propionate accumulation was one of the major reasons for the pH drop and inhibition of methanogenesis [30,31]. Its high concentration in the biochar-D reactor led to its system instability and low methane production. Overall, the addition of biochar led to faster and more stable production of methane, and consumption of VFAs by microbes maintained the pH in a moderate range, eventually benefitting methanogenesis.

The GC–MS results supported the aforementioned trend (Fig. 5A). The results showed that the addition of biochar (except for biochar-D) successfully removed acid derivatives and amide derivatives. Fig. 5A also presents the removal efficiencies of some other micromolecular organics in HTL-AP with the addition of biochar and GAC, and several of these compounds are aromatic and nitrogen-containing compounds that could inhibit anaerobic digestion. The overall result showed that most of the inhibitory compounds could be degraded by more than 80%, but a large fraction of the nitrogen heterocyclic compounds, such as pyridine and pyrrolidine derivatives, remained in the reactor after digestion. Meanwhile, biochar-D provided a weaker boost to the removal of micro-organics in the actual HTL-AP than the other types of biochar, which was consistent with the phenol, pyridine, and hydroxypyridine adsorption results. For example, the removal efficiency of phenol, 4-methyl-phenol, 2-piperidinone, and 6-methyl-3-pyridinol were 10.6%, 81.7%, 5.3%, and 30.7% lower than other biochar-amended groups, respectively. Differences between groups can be observed more clearly in the organic conversion results of the macromolecules presented in Fig. 5B. Compared to the representative micro-organics in Fig. 5A, the MALDI analysis in Fig. 5B shows a more comprehensive picture of organic conversion. The vast majority of organic substances in HTL-AP have molecular weights less than 1000 Da, while biopolymers (>20 kDa), such as high molecular weight polysaccharides and protein-like substances, are also present [32]. It's reasonable to observe negative organic removal because some of the macromolecules degraded from high molecular weight compounds were not completely converted to gas products, and therefore remained in the aqueous phase after digestion. The results in Fig. 5B show that biochar-E addition provided the best organic removal, and most of the organic matter was converted into gas products. The decomposition of macromolecular compounds was reported to be related to enhanced hydrolysis with biochar addition. For example, Duan et al. (2019) reported that biochar stimulated the increase of functional genes and the activation of several hydrolases, including protease, dextranase, and lipase, which contributed to enhanced hydrolysis [33]. This result confirmed the positive effects of biochar addition on the enrichment of acid-forming bacteria and degradation of macro-organics. In contrast, the removal was not efficient with biochar-D, which manifested in many macromolecules, as well as micro-molecules, remaining after digestion. The organic removal differences can be attributed to the inherent properties of added biochar. The great adsorption capacity of biochar facilitated the adsorption of organic matter, especially toxic cyclic and nitrogen-containing compounds during digestion. Meanwhile, its abundant porous structure benefited the attachment and growth of different microorganisms, helped biofilm formation, and promoted microbial interactions. The digestion process of HTL-AP was complex, and organic degradation occurred at the same time as adsorption. Subtle differences in biochar structure can lead to a different conversion performance.

Although the result in Fig. 5 showed that biochar-E had a comparable organic removal performance with that of GAC. It is worth noting that there is still a gap between biochar-E and GAC in terms of COD removal. This discrepancy indicated that although biochar-E was good at dealing with organic compounds, GAC was much better at eliminating inorganic compounds, and its overall efficiency was significantly higher than the biochar groups. Nonetheless, considering the overall organic conversion and methane production efficiency, biochar-E still can be an ideal additive to facilitate anaerobic digestion.

3.4. Biochar addition affects microbial enrichment and metabolic pathways

The different effects of biochar on methane production and organic conversion indicated the differences in metabolic interactions within microbial communities. Results of microbial analysis confirmed that the composition and content of microorganisms within reactors varied. The principal component analysis (PCA) of microbial composition in different reactors exhibited an obvious separation between biochar-D and other groups, as shown in Fig. 6. Fig. 6B demonstrates microbial aggregation based on bacteria families. Results showed that reactors

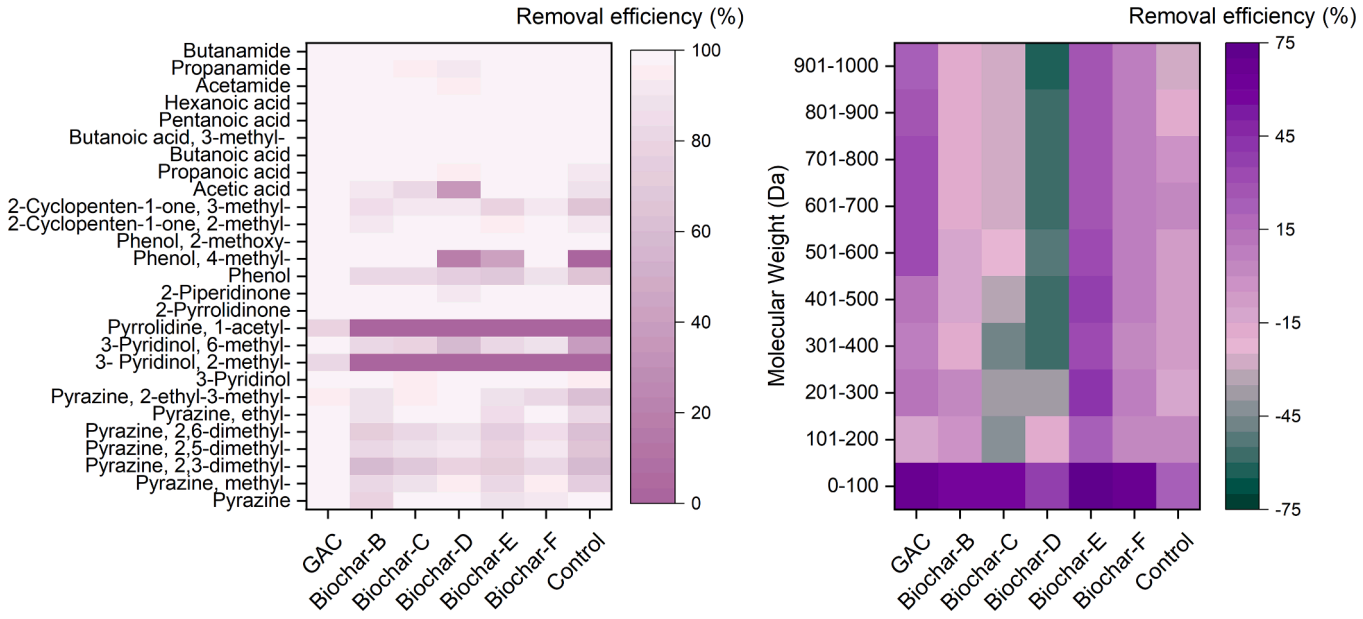

Fig. 5. Organic conversion efficiency of representative compounds (A) and overall organic removal performance (B) with different biochar addition.

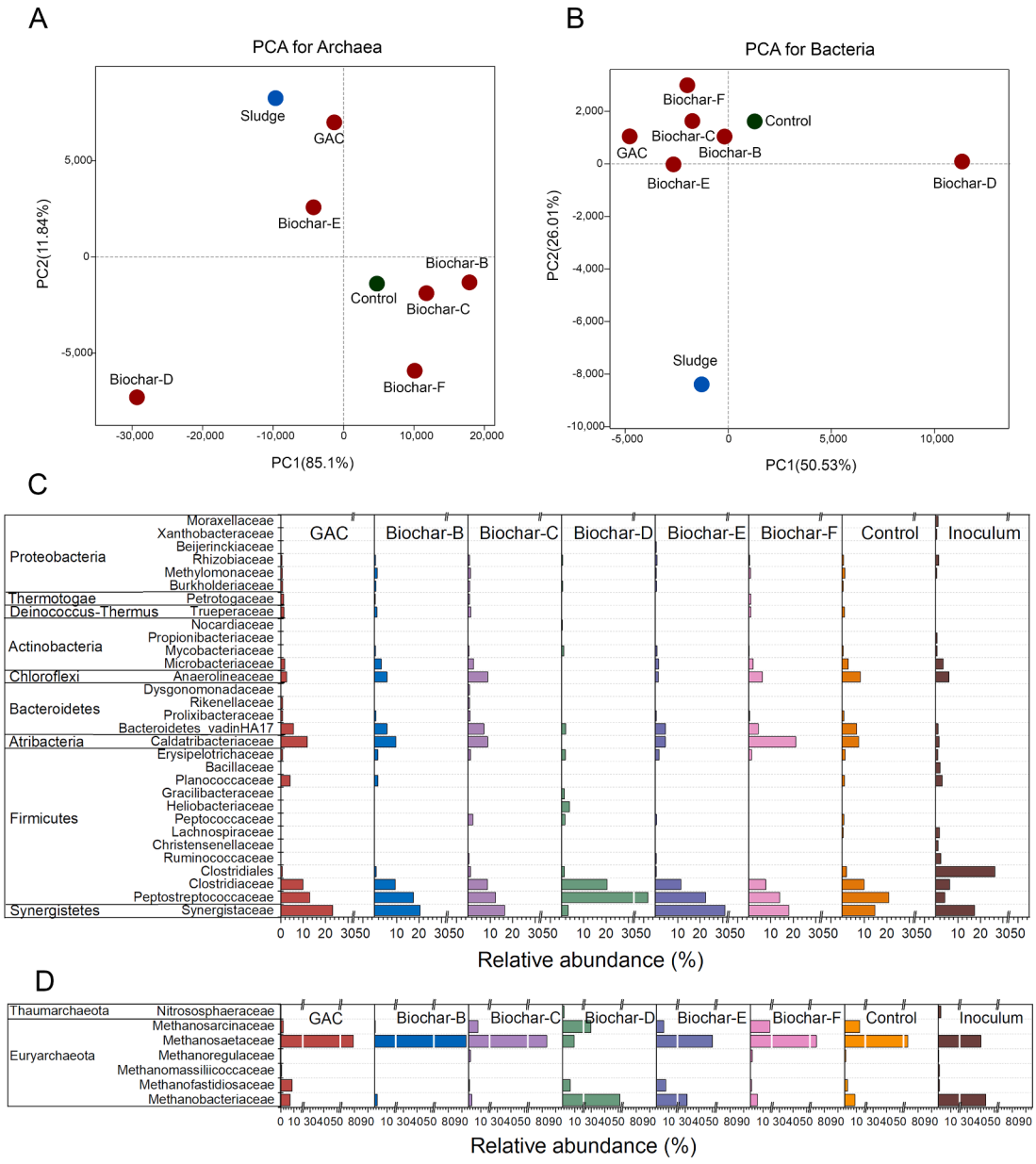

Fig. 6. PCA analysis of archaeal (A) and bacterial (B) composition with different biochar addition. Relative abundance of bacteria (C) and archaea (D). The cutoff line for the selected microbes was no less than 0.5% of the total composition.

amended with biochar-E, biochar-C, biochar-F, and biochar-B had similar microbial compositions as the GAC-assisted reactor. However, the digester with biochar-D addition had a significantly different microbial structure. However, the microbial aggregation based on archaea was relatively dispersed (Fig. 6A). Biochar-E addition showed a similar effect as GAC on microbial composition while biochar-B, biochar-C, and biochar-F were grouped together. Biochar-D had a different pattern, which was also consistent with the differences in relative abundance. These results comprehensively indicated that the difference in methane production could be attributed to the difference in the microbial community and syntrophic interactions. Inhibition in methane generation with biochar-D addition suggested that biochar could perform both positive and negative effects on methanogenesis during anaerobic digestion.

The number of operational taxonomic units (OTUs) for different reactors reflected the diversity of microbial communities. Among the biochar amended reactors, biochar-D-assisted digestion had the lowest microbial diversity with 512 microbial OTUs and 60 archaeal OTUs, which was maximally 357 microbial and 31 archaeal OTUs less than other groups. This low microbial diversity resulted in the lowest capacity of biochar-D to resist environmental stress and maintain system stability.

The most abundant bacteria belonged to the phylum *Synergistetes*, *Firmicutes*, *Atribacteria*, *Bacteroidetes*, *Chloroflexi*, *Actinobacteria*, *Deinococcus-Thermus*, *Thermotogae*, and *Proteobacteria* (Fig. 6C). Enrichment of the bacterial population with different biochar and GAC varied. For biochar-B, C, E, and F, the most dominant bacteria they raised was the *Thermovirga* genus under the *Synergistaceae* family and *Synergistetes* phylum. The abundance of *Thermovirga* in the biochar-E amended reactor was 30.7%, which was 2.2 and 1.4 times higher than the control and GAC-assisted reactor, respectively. However, the abundance of *Thermovirga* enriched by biochar-D was only 3.1%, which was even much lower than that of the control (14.2%). These results implied that biochar addition stimulated the enrichment of *Thermovirga* and led to a different microbial composition. The primary function of *Thermovirga* was reported to be amino-acid degradation; it could ferment proteinous

substances, certain single amino acids, and certain organic acids. The end products could be acetate, propionate, ethanol, H_2, CO_2, etc. [34]. *Thermovirga* possesses a flagella structure that allows for electron transfer [34,35], while no direct evidence is available for its involvement in DIET. It is still possible that DIET was established between *Thermovirga* and methanogens, but it would not be the primary mechanism because the electrical conductivity of both sludge and biochar was low. It is more likely that *Thermovirga* acts as an acidogenic bacteria accelerating hydrolysis/acidogenesis, COD removal, and methane generation, which has been reported in several other anaerobic systems [36–38].

Another bacteria exhibiting different dominant patterns is the *Candidatus Caldatribacterium* genus under the *Caldatribacteriaceae* family and the *Atribacteria* phylum. The abundance of *Candidatus Caldatribacterium* in a reactor with biochar-D was less than 0.1%, while the content in biochar-F was 21.1% of the total composition. *Candidatus Caldatribacterium* was characterized as a hydrogen and acid producer from carbohydrate fermentation [39–41], and the flagellar genes found in *Candidatus Caldatribacterium* suggested its potential for electron transfer [41]. However, biochar-induced enrichment was not always overwhelming. Its abundance in biochar-B, biochar-C, GAC, and control reactors were 9.8%, 8.9%, 11.9%, and 7.6% respectively. Its abundance in the biochar-E reactor (4.5%) was even lower than the control (7.6%), which contradicts the highest methane yield in the biochar-E group. These results suggest that *Candidatus Caldatribacterium* can be enriched by certain biochar and act as an acidogen to promote organic conversion, but it is not the key functional bacterium for enhanced digestion.

Moreover, the *Anaerolineaceae* family under the *Chloroflexi* phylum was the dominant bacteria that did not appear in biochar-D assisted digestion, but it was abundant in other reactors, especially with the inclusion of biochar-C (8.9%). Although its certain role in anaerobic digestion has not been clarified, *Anaerolineaceae* demonstrated great metabolic ability for carbohydrate degradation, and the end products could be acetate, lactate, hydrogen, formate, etc. [42,43]. Notably, *Anaerolineaceae* proved to be related to phenol degradation, and it could maintain an efficient degradation efficiency even under high phenol inhibition conditions [44]. The different *Anaerolineaceae* abundance was consistent with the organic removal results that biochar-D exhibited the worst conversion of phenol derivatives (Fig. 5A), and the adsorption tests also demonstrated that phenol derivatives could not be effectively adsorbed by biochar-D (Fig. 3). Enrichment of *Anaerolineaceae* by biochar stimulation has also been reported by Wang et al., and they speculated that it might function as an electron donor and participate in DIET [11]. However, Xia et al. found that the pili structure of *Anaerolineaceae* contributed to cellular adhesiveness and aggregation rather than syntrophic methanogenesis via DIET [42]. Here, the fact that the *Anaerolineaceae* abundance in the non-amended control reactor (8.3%) was higher than that in biochar-B, biochar-E, biochar-F, and GAC ruled out the possibility of a syntrophic interaction between *Anaerolineaceae* and methanogens.

As for the microbial community enriched with biochar-D, the most dominant bacteria was the *Asaccharospora* genus under the *Peptostreptococcaceae* family and the *Firmicutes* phylum with a relative abundance of 32.1%. While the abundances in other reactors were no more than 10.6%. It was reported that *Asaccharospora* could not utilize any type of carbohydrates when the major organic metabolite was acetate [45]. This property may help explain the deficiency in biological degradation with biochar-D. Following *Asaccharospora*, the *Clostridium* genus under the *Clostridiaceae* family showed a dominant presence (19.1%) in the biochar-D amended reactor, which was about 2 times higher than other reactors in the total microbial composition. *Clostridium* could degrade cellulosic compounds. The main product was acetate while formate could also be formed. It was also reported to participate in syntrophic acetate oxidation (SAO) with hydrogenotrophic methanogens for hydrogen production [46–49]. With a flagella structure, *Clostridium* has been reported to participate in the DIET process as an electron donor [50–52]. The possibility of DIET existence cannot be ruled out here, but the sludge conductivity remained at a low level (Table 3), indicating that the conductive pili structure for DIET establishment was not significantly enriched. Therefore, mediated interspecies electron transfer via hydrogen and formate would still be the main mechanism via *Clostridium* and methanogens. These two major bacteria accounted for more than half of the microbial abundance in the biochar-D assisted reactor, and its microbial diversity was lower than in other groups. This deficiency is very likely to be responsible for its poor organic degradation and methane generation performance. Shao et al. reported that biochar addition could help the attachment and colonization of bacteria competing for hydrogen and reduce the amount of hydrogen available for hydrogenotrophic methanogens, thereby weakening methanogenesis [53]. Here, it's possible that some of the enriched bacteria consumed hydrogen and prevented methanogens from producing methane in the biochar-D amended reactors.

In terms of archaea, the most abundant species belonged to the family *Nitrososphaeraceae*, *Methanosarcinaceae*, *Methanosaetaceae*, *Methanoregulaceae*, *Methanomassiliicoccaceae*, *Methanofastidiosaceae*, and *Methanobacteriaceae* (Fig. 6D). Among these microbes, the *Methanosaeta* genus under the *Methanosaetaceae* family was the most dominant for all reactors (more than 50% of the total composition) except for biochar-D addition (9.5%), and it reached the highest abundance with biochar-B addition (93.2%). The abundance of *Methanosaeta* in the non-amended control reactor was 2.5%-29.0% lower than with biochar addition, demonstrating that biochar enriched the archaeal population. Nevertheless, biochar-D addition led to a shift in dominance from *Methanosaeta* to *Methanobacterium* (49.8%, *Methanobacteriaceae* family) and *Methanosarcina* (29.6%, *Methanosarcinaceae* family). *Methanosaeta* is an acetoclastic methanogen, while *Methanobacterium* is a hydrogenotrophic methanogen, and *Methanosarcina* is capable of all three major methanogenic pathways (hydrogenotrophic, acetoclastic, and methylotrophic). The different microbial compositions suggested that SAO coupled to hydrogenotrophic methanogenesis might be the primary pathway stimulated by biochar-D, while acetoclastic methanogenesis dominated in other reactors. This result is also consistent with the accumulation of VFAs in which acetate and propionate accumulated for a longer time and a higher concentration in the biochar-D reactor since *Methanobacterium* played an important role in propionate degradation and *Methanosarcina* tended to be enriched over *Methanosaeta* with a high acetate concentration [54,55]. The hydrogenotrophic process is highly affected by the hydrogen concentration, and the lowered methane yield of biochar-D might be due to the insufficient efficiency of hydrogen-mediated interspecies electron transfer. Notably, the abundance of *Methanobacterium* was also considerable (26.2%) in addition to the dominant *Methanosaeta* (50.2%) for biochar-E, demonstrating that acetoclastic and hydrogenotrophic methanogenesis were both active and favored the overall organic utilization.

The morphologies of the enriched microbes on different biochars varied with the different microbial compositions (Fig. A.2). Microbes were attached and aggregated on the biochar surface, and most of them were rod-shaped, which is consistent with the fact that most of the dominant microbes were rod-shaped. Different aggregation patterns were observed between groups. For example, the aggregation on the biochar-F surface was more intensive than the other groups, which might be related to the specific aggregation characteristics of its dominant microbe *Candidatus Caldatribacterium* (Fig. 6C). It was also found that the biochar-B had more small-sized microbes attached to its surface. This may be explained by the fact that the smaller pore volume of biochar-B favored the enrichment of small microbes to help more microbes attach to its surface for metabolism, while the large-sized microbes were less enriched.

The aforementioned analysis revealed that different types of biochar addition stimulated different metabolic responses in the microbial community, which subsequently led to the difference in organic conversion. Acidogenesis, acetogenesis, and methanogenesis can all be

greatly enhanced with biochar induction, but no clear evidence points to the domination of DIET.

3.5. Correlation analysis and model prediction

3.5.1. Correlation analysis of biochar addition with anaerobic digestion of HTL-AP

A comprehensive correlation analysis between biochar properties and microbial activity as well as methane production is presented in Fig. 7 (only dominant microbes; the full correlation plot can be found in Fig. A.3. The result shows that total pore volume was negatively related to methane yield and production rate, while positively correlated to the lag phase, indicating that an excessively large pore volume may be detrimental. This finding was validated by the microbial composition which demonstrated that a larger total pore volume helped the enrichment of biochar-D associated microbes while it was unfavorable for others. Moreover, the adsorption capacities were highly related to both methane generation and microbial enrichment, proving that biochar promoted microbial growth and metabolism by adsorption of toxic inhibitory substances, thereby improving digestion. Elemental composition could also be influential, especially the O/C ratio. With a higher O/C ratio, the higher adsorption capacity of biochar for heavy metals can be achieved. It was also found that although the surface area had a limited effect on methane production, it can be associated with microbial abundance. This is reasonable because more connection sites were provided for microbial attachment with a larger biochar surface. Electrical conductivity, electron-donating capacity, and electron-accepting capacity had negligible effects on most microbes, and similarly, had limited effects on methane production.

In addition to its intrinsic properties, the effects of biochar addition on the system have been analyzed. As an alkaline material, biochar addition helps neutralize the pH value within anaerobic digesters, avoids reactor souring due to the accumulation of organic acids, and further contributes to system stability [5]. Thus, the initial and final pH values were monitored, and results showed that the final pH values of all reactors increased and remained at a similar level (pH = 7.4–7.6) (Fig. A.4). The consistent final pH in all reactors demonstrated that the difference in methane yield was not attributed to the pH variations. The ammonia concentration was also monitored (Fig. A.4) and its value in all reactors was not so high as to induce inhibition of digestion (>1500 mg/L) [56], confirming that the difference in methanogenesis was not attributed to the ammonia variation with biochar addition.

These findings demonstrated that pore volume and adsorption capacities were the determining parameters of biochar, which affected the system environment and microbial metabolism, eventually reflected in the differences in organic conversion and biogas yield. Meanwhile, although it is possible that biochar addition stimulated the co-existence of DIET with mediated interspecies electron transfer, the low electrical conductivity and electron transfer capacity of biochar, as well as the low sludge conductivity, limited its domination. Mediated interspecies electron transfer via hydrogen and formate should still be the primary mechanism over DIET.

3.5.2. Model predictions on DIET establishment with biochar properties

To further investigate the relationship between biochar properties and DIET existence, a Random Forest model was built to predict and validate the results obtained in this study. 23 data points collected from previous studies (Table A.2) were used as training data to predict the binomial response for the presence of DIET, and 9 parameters (surface area, conductivity, pore volume, electron-donating capacity, electron-accepting capacity, carbon, nitrogen, oxygen, and hydrogen content) were used as independent variables. PCA analysis was performed to compare how much each variable contributed to the main variance in the dataset, and Fig. 8 visualizes the relationship among variables with different response groups (DIET exists or does not exist). Results showed that the first 2 principal components explained 60.8% of the variance, and pore volume and electron-donating capacity caused the greatest variance. Fig. 8 also shows that the presence of DIET can be characterized by pore volume, surface area, conductivity, as well as the content of carbon and hydrogen. This conclusion is convincing because pore volume and surface area influence microbial adhesion, and conductivity and the H/C ratio are both related to the electron transfer of microbes through biochar. To evaluate the ability of this model to predict the presence of DIET, the out-of-bag (OOB) error rate was checked with a value of 13%, indicating a model accuracy of 87%. Moreover, 3 of the 5 biochar addition groups in the present study were predicted as DIET not

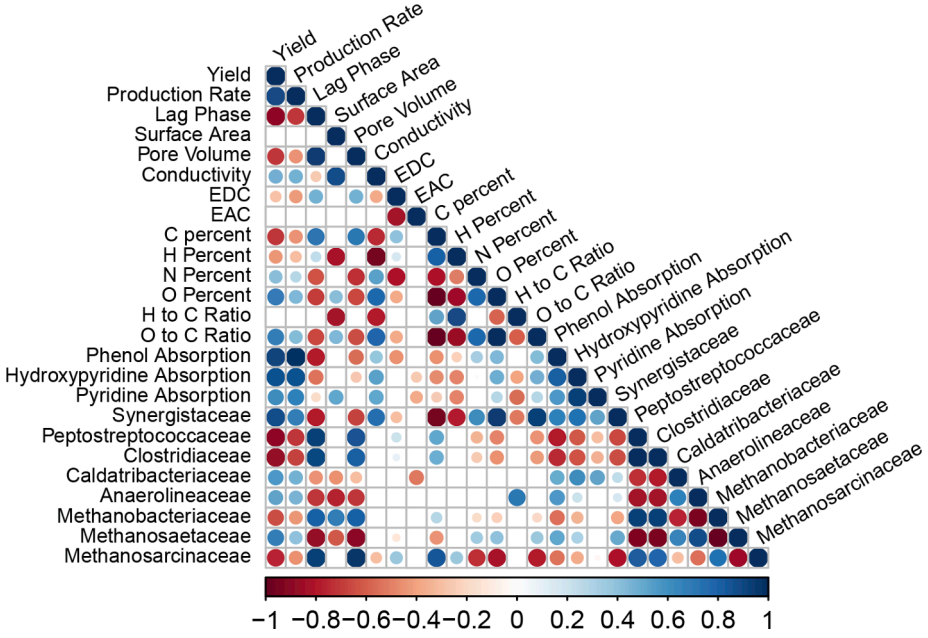

Fig. 7. Correlation plot of biochar properties (data from biochar-B, C, D, E, and F) with methane production and microbial activity (only dominant microbes; the full correlation plot is shown in Fig. A.3; positive correlations are in red while negative correlations are in blue). EDC: electron-donating capacity, EAC: electron-accepting capacity.

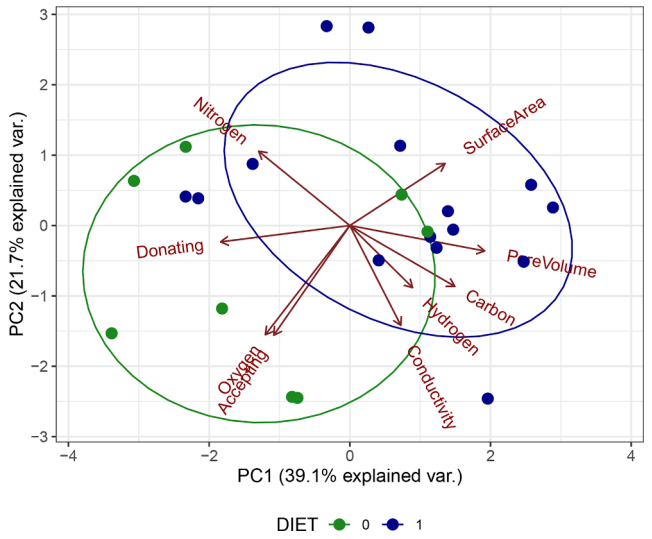

Fig. 8. PCA analysis indicating the relationship among variables of biochar with the different responses of DIET. 0 means DIET does not exist, and 1 means DIET exists. Donating and accepting indicate the electron-donating/accepting capacity. Nitrogen, oxygen, carbon, and hydrogen indicate their contents in biochar.

being established/dominated by this model. The accuracy and precision of the current model are not very high, and the prediction error was mainly caused by the dataset itself. Although the data points were carefully selected from the literature with more reliable evidence, the effect of a small sample size on the model accuracy is still unavoidable. The missing values in the data are another factor that affected the model. Nevertheless, these results could still provide a qualitative corroboration indicating whether the addition of biochar in anaerobic digestion makes DIET dominant. The relationship between biochar and DIET is complex, and some potential connections may not have been identified. The modeling approach can help to better understand the whole process and find some key points that have been overlooked. Furthermore, the accuracy of this model can be further improved as more studies are published and more abundant, accurate data becomes available.

4. Conclusions and implications

This study investigated the effects of different biochar additions on methane production during anaerobic digestion of HTL-AP. In most cases, adding biochar could facilitate organic removal and methanogenesis. Total pore volume and adsorption capacity of biochar proved to be the determining factors as they led to an improvement in the microbial community structure and activity. However, adding biochar was not always beneficial. A suppressive biochar (biochar-D) addition could induce a shifted microbial composition and metabolic pathways which were different from the non-amended control reactor, accounting for suppressed methane generation.

The poor conductivity and electron transfer capacity of biochar limited its role as an electron conduit for DIET. Furthermore, the low sludge conductivity indicated that the conductive pili were not significantly enriched, although some dominant microbes had the capability of transferring electrons. These findings demonstrated that mediated interspecies electron transfer was still the primary mechanism for electron transfer, but the possibility of DIET being present was not ruled out. The results also suggested that the relationship between DIET and biochar should be further investigated. For example, the selection of raw materials and the subsequent processing conditions can influence the properties of biochar and affect its ability to induce DIET. Considering each biochar parameter (pore volume, conductivity, electron transfer capacity, surface area, etc.) and testing their effects on DIET individually could lead to more discoveries about their relationships. Genomic and transcriptomic analyses should also be conducted in future studies to monitor the changes in pili/cytochrome structures, as well as associated metabolic processes, to provide more direct evidence for the presence of DIET. Moreover, the establishment of DIET with biochar may also be substrate-related. Ethanol could be considered as a co-substrate to stimulate the biological connection to achieve DIET, as it has been proven to be an effective electron donor for DIET [13,57,58]. Modification of biochar would be another promising strategy. For example, magnetite or nitrogen-doped biochar may help establish DIET by improving its electrical conductivity and capacitance [59,60]. This study also developed a prediction model to relate DIET with biochar properties with a model accuracy of 87%, providing qualitative support for determining whether the role of biochar in anaerobic digestion was DIET-dominant. In future studies, more statistical and modeling approaches could be applied, which will likely provide more insight into the induction mechanisms and help find suitable biochar for digestion.

Declaration of Competing Interest

The authors declare that they have no known competing financial interests or personal relationships that could have appeared to influence the work reported in this paper.

Acknowledgment

This work was supported by the National Science Foundation (NSF CBET 18-04453); the National Natural Science Foundation of China (NSFC 51806243); and the China Scholarship Council Grant (#201908040007).

Appendix A. Supplementary data

Supplementary data to this article can be found online at https://doi.org/10.1016/j.cej.2022.135078.

References

[1] A. Aierzhati, J. Watson, B. Si, M. Stablein, T. Wang, Y. Zhang, Development of a mobile, pilot scale hydrothermal liquefaction reactor: Food waste conversion product analysis and techno-economic assessment, Energy Convers. Manag. X. 10 (2021) 100076. /10.1016/j.ecmx.2021.100076.
[2] J. Watson, B. Si, Z. Wang, T. Wang, A. Valentine, Y. Zhang, Towards transportation fuel production from food waste: Potential of biocrude oil distillates for gasoline, diesel, and jet fuel, Fuel. 301 (2021) 121028. /10.1016/j.fuel.2021.121028.
[3] J. Watson, T. Wang, B. Si, W.-T. Chen, A. Aierzhati, Y. Zhang, Valorization of hydrothermal liquefaction aqueous phase: pathways towards commercial viability, Prog. Energy Combust. Sci. 77 (2020) 100819, https://doi.org/10.1016/j.pecs.2019.100819.
[4] B. Si, L. Yang, X. Zhou, J. Watson, G. Tommaso, W.T. Chen, Q. Liao, N. Duan, Z. Liu, Y. Zhang, Anaerobic conversion of the hydrothermal liquefaction aqueous phase: Fate of organics and intensification with granule activated carbon/ozone pretreatment, Green Chem. 21 (2019) 1305–1318. /10.1039/c8gc02907e.
[5] S. Tang, Z. Wang, Z. Liu, Y. Zhang, B. Si, The role of biochar to enhance anaerobic digestion: A review, J. Renew. Mater. 8 (2020) 1033–1052. /10.32604/jrm.2020.011887.
[6] M. Chiappero, O. Norouzi, M. Hu, F. Demichelis, F. Berruti, F. Di Maria, O. Mašek, S. Fiore, Review of biochar role as additive in anaerobic digestion processes, Renew. Sustain. Energy Rev. 131 (2020). /10.1016/j.rser.2020.110037.
[7] M.O. Fagbohungbe, B.M.J. Herbert, L. Hurst, C.N. Ibeto, H. Li, S.Q. Usmani, K.T. Semple, The challenges of anaerobic digestion and the role of biochar in optimizing anaerobic digestion, Waste Manag. 61 (2017) 236–249. /10.1016/j.wasman.2016.11.028.
[8] J. Wang, S. Wang, Preparation, modification and environmental application of biochar: A review, J. Clean. Prod. 227 (2019) 1002–1022. /10.1016/j.jclepro.2019.04.282.
[9] G. Wang, X. Gao, Q. Li, H. Zhao, Y. Liu, X.C. Wang, R. Chen, Redox-based electron exchange capacity of biowaste-derived biochar accelerates syntrophic phenol oxidation for methanogenesis via direct interspecies electron transfer, J. Hazard. Mater. 390 (2020), 121726, https://doi.org/10.1016/j.jhazmat.2019.121726.
[10] Q. Qi, C. Sun, J. Zhang, Y. He, Y. Wah Tong, Internal enhancement mechanism of biochar with graphene structure in anaerobic digestion: The bioavailability of trace elements and potential direct interspecies electron transfer, Chem. Eng. J. 406 (2021) 126833. /10.1016/j.cej.2020.126833.

[11] G. Wang, Q. Li, X. Gao, X.C. Wang, Synergetic promotion of syntrophic methane production from anaerobic digestion of complex organic wastes by biochar: Performance and associated mechanisms, Bioresour. Technol. 250 (2018) 812–820. /10.1016/j.biortech.2017.12.004.
[12] C. Wang, Y. Liu, X. Gao, H. Chen, X. Xu, L. Zhu, Role of biochar in the granulation of anaerobic sludge and improvement of electron transfer characteristics, Bioresour. Technol. 268 (2018) 28–35. /10.1016/j.biortech.2018.07.116.
[13] A.E. Rotaru, P.M. Shrestha, F. Liu, M. Shrestha, D. Shrestha, M. Embree, K. Zengler, C. Wardman, K.P. Nevin, D.R. Lovley, A new model for electron flow during anaerobic digestion: Direct interspecies electron transfer to Methanosaeta for the reduction of carbon dioxide to methane, Energy Environ. Sci. 7 (2014) 408–415. /10.1039/c3ee42189a.
[14] Z.M. Summers, H.E. Fogarty, C. Leang, A.E. Franks, N.S. Malvankar, D.R. Lovley, Direct exchange of electrons within aggregates of an evolved syntrophic coculture of anaerobic bacteria, Science (80-) 330 (6009) (2010) 1413–1415.
[15] M. Morita, N. Malvankar, A. Franks, Z. Summers, L. Giloteaux, A. Rotaru, C. Rotaru, D. Lovley, Potential for direct interspecies electron transfer in methanogenic, MBio 2 (2011) 5–7, https://doi.org/10.1128/mBio.00159-11. Editor.
[16] Z. Wang, T. Wang, B. Si, J. Watson, Y. Zhang, Accelerating anaerobic digestion for methane production: Potential role of direct interspecies electron transfer, Renew. Sustain. Energy Rev. 145 (2021) 111069. /10.1016/j.rser.2021.111069.
[17] S. Ren, M. Usman, D.C.W. Tsang, S. O-Thong, I. Angelidaki, X. Zhu, S. Zhang, G. Luo, Hydrochar-Facilitated Anaerobic Digestion: Evidence for Direct Interspecies Electron Transfer Mediated through Surface Oxygen-Containing Functional Groups, Environ. Sci. Technol. 54 (2020) 5755–5766. /10.1021/acs.est.0c00112.
[18] C.C. Viggi, S. Simonetti, E. Palma, P. Pagliaccia, C. Braguglia, S. Fazi, S. Baronti, M. A. Navarra, I. Pettiti, C. Koch, F. Harnisch, F. Aulenta, Enhancing methane production from food waste fermentate using biochar: The added value of electrochemical testing in pre-selecting the most effective type of biochar, Biotechnol. Biofuels 10 (2017) 1–13, https://doi.org/10.1186/s13068-017-0994-7.
[19] C. Lü, Y. Shen, C. Li, N. Zhu, H. Yuan, Redox-Active Biochar and Conductive Graphite Stimulate Methanogenic Metabolism in Anaerobic Digestion of Waste-Activated Sludge: Beyond Direct Interspecies Electron Transfer, ACS Sustain. Chem. Eng. 8 (2020) 12626–12636. /10.1021/acssuschemeng.0c04109.
[20] E. Meschewski, N. Holm, B.K. Sharma, K. Spokas, N. Minalt, J.J. Kelly, Pyrolysis biochar has negligible effects on soil greenhouse gas production, microbial communities, plant germination, and initial seedling growth, Chemosphere. 228 (2019) 565–576. /10.1016/j.chemosphere.2019.04.031.
[21] L. Klüpfel, M. Keiluweit, M. Kleber, M. Sander, Redox properties of plant biomass-derived black carbon (biochar), Environ. Sci. Technol. 48 (2014) 5601–5611. /10.1021/es500906d.
[22] B. Si, Z. Liu, Y. Zhang, J. Li, R. Shen, Z. Zhu, X. Xing, Towards biohythane production from biomass: Influence of operational stage on anaerobic fermentation and microbial community, Int. J. Hydrogen Energy. 41 (2016) 4429–4438. /10.1016/j.ijhydene.2015.06.045.
[23] M.F. Altamirano-Corona, O. Anaya-Reza, A. Durán-Moreno, Biostimulation of food waste anaerobic digestion supplemented with granular activated carbon, biochar and magnetite: A comparative analysis, Biomass Bioenergy 149 (2021). /10.1016/j.biombioe.2021.106105.
[24] T.M. Huggins, A. Haeger, J.C. Biffinger, Z.J. Ren, Granular biochar compared with activated carbon for wastewater treatment and resource recovery, Water Res. 94 (2016) 225–232. /10.1016/j.watres.2016.02.059.
[25] Z. Yang, T. Sun, E. Subdiaga, M. Obst, S.B. Haderlein, M. Maisch, R. Kretzschmar, L.T. Angenent, A. Kappler, Aggregation-dependent electron transfer via redox-active biochar particles stimulate microbial ferrihydrite reduction, Sci. Total Environ. 703 (2020) 135515. /10.1016/j.scitotenv.2019.135515.
[26] Keiluweit, P.S. Nico, M. Johnson, M. Kleber, Dynamic molecular structure of plant biomass-derived black carbon (biochar), Environ. Sci. Technol. 44 (2010) 1247–1253. /10.1021/es9031419.
[27] M. Ahmad, S.S. Lee, X. Dou, D. Mohan, J.K. Sung, J.E. Yang, Y.S. Ok, Effects of pyrolysis temperature on soybean stover- and peanut shell-derived biochar properties and TCE adsorption in water, Bioresour. Technol. 118 (2012) 536–544. /10.1016/j.biortech.2012.05.042.
[28] L. Wei, Y. Huang, L. Huang, Y. Li, Q. Huang, G. Xu, K. Müller, H. Wang, Y.S. Ok, Z. Liu, The ratio of H/C is a useful parameter to predict adsorption of the herbicide metolachlor to biochars, Environ. Res. 184 (2020) 109324, https://doi.org/10.1016/j.envres.2020.109324.
[29] Q. Li, X. Gao, Y. Liu, G. Wang, Y.Y. Li, D. Sano, X. Wang, R. Chen, Biochar and GAC intensify anaerobic phenol degradation via distinctive adsorption and conductive properties, J. Hazard. Mater. 405 (2021) 124183. /10.1016/j.jhazmat.2020.124183.
[30] M. Mösche, H.-J. Jördening, Comparison of different models of substrate and product inhibition in anaerobic digestion, Water Res. 33 (11) (1999) 2545–2554.
[31] J. Li, Q. Ban, L. Zhang, A.K. Jha, Syntrophic propionate degradation in anaerobic digestion: A review, Int. J. Agric. Biol. 14 (2012) 843–850.
[32] S. Hao, S. Ren, N. Zhou, H. Chen, M. Usman, C. He, Q. Shi, G. Luo, S. Zhang, Molecular composition of hydrothermal liquefaction wastewater from sewage sludge and its transformation during anaerobic digestion, J. Hazard. Mater. 383 (2020) 121163. /10.1016/j.jhazmat.2019.121163.
[33] X. Duan, Y. Chen, Y. Yan, L. Feng, Y. Chen, Q. Zhou, New method for algae comprehensive utilization: Algae-derived biochar enhances algae anaerobic fermentation for short-chain fatty acids production, Bioresour. Technol. 289 (2019) 121637. /10.1016/j.biortech.2019.121637.
[34] H. Dahle, N.K. Birkeland, Thermovirga lienii gen. nov., sp. nov., a novel moderately thermophilic, anaerobic, amino-acid-degrading bacterium isolated from a North Sea oil well, Int. J. Syst. Evol. Microbiol. 56 (2006) 1539–1545. /10.1099/ijs.0.63894-0.
[35] M. Göker, E. Saunders, A. Lapidus, M. Nolan, S. Lucas, N. Hammon, S. Deshpande, J.F. Cheng, C. Han, R. Tapia, L.A. Goodwin, S. Pitluck, K. Liolios, K. Mavromatis, I. Pagani, N. Ivanova, N. Mikhailova, A. Pati, A. Chen, K. Palaniappan, M. Land, Y. J. Chang, C.D. Jeffries, E.M. Brambilla, M. Rohde, S. Spring, J.C. Detter, T. Woyke, J. Bristow, J.A. Eisen, V. Markowitz, P. Hugenholtz, N.C. Kyrpides, H.P. Klenk, Genome sequence of the moderately thermophilic, amino-acid-degrading and sulfur-reducing bacterium Thermovirga lienii type strain (Cas60314T), Stand. Genomic Sci. 6 (2012) 230–239, https://doi.org/10.4056/sigs.2726028.
[36] K. Venkiteshwaran, K. Milferstedt, J. Hamelin, D.H. Zitomer, Anaerobic digester bioaugmentation influences quasi steady state performance and microbial community, Water Res. 104 (2016) 128–136. /10.1016/j.watres.2016.08.012.
[37] L. Luo, S. Xu, Y. Jin, R. Han, H. Liu, F. Lü, Evaluation of methanogenic microbial electrolysis cells under closed/open circuit operations, Environ. Technol. (United Kingdom). 39 (2018) 739–748. /10.1080/09593330.2017.1310934.
[38] S. wen Du, C. Sun, A. qiang Ding, W. wang Chen, M. jie Zhang, R. Cheng, D. lei Wu, Microbial dynamics and performance in a microbial electrolysis cell-anaerobic membrane bioreactor, J. Zhejiang Univ. Sci. A. 20 (2019) 533–545. /10.1631/jzus.A1900009.
[39] T. Ao, R. Li, Y. Chen, C. Li, Z. Li, X. Liu, Y. Ran, D. Li, Anaerobic thermophilic digestion of maotai-flavored distiller's grains: process performance and microbial community dynamics, Energy Fuels 33 (2019) 8804–8811. /10.1021/acs.energyfuels.9b02582.
[40] N. Zamorano-López, S. Greses, D. Aguado, A. Seco, L. Borrás, Thermophilic anaerobic conversion of raw microalgae: Microbial community diversity in high solids retention systems, Algal Res. 41 (2019) 101533. /10.1016/j.algal.2019.101533.
[41] J.A. Dodsworth, P.C. Blainey, S.K. Murugapiran, W.D. Swingley, C.A. Ross, S. G. Tringe, P.S.G. Chain, M.B. Scholz, C.C. Lo, J. Raymond, S.R. Quake, B. P. Hedlund, Single-cell and metagenomic analyses indicate a fermentative and saccharolytic lifestyle for members of the OP9 lineage, Nat. Commun. 4 (2013), https://doi.org/10.1038/ncomms2884.
[42] Y. Xia, Y. Wang, Y. Wang, F.Y.L. Chin, T. Zhang, Cellular adhesiveness and cellulolytic capacity in Anaerolineae revealed by omics-based genome interpretation, Biotechnol. Biofuels 9 (2016) 1–13. /10.1186/s13068-016-0524-z.
[43] T. Yamada, Y. Sekiguchi, S. Hanada, H. Imachi, A. Ohashi, H. Harada, Y. Kamagata, Anaerolinea thermolimosa sp. nov., Levilinea saccharolytica gen. nov., sp. nov. and Leptolinea tardivitalis gen. nov., sp. nov., novel filamentous anaerobes, and description of the new classes Anaerolineae classis nov. and Caldilineae classis nov. in the bacterial phylum Chloroflexi, Int. J. Syst. Evol. Microbiol. 56 (2006) 1331–1340, https://doi.org/10.1099/ijs.0.64169-0.
[44] F. Rosenkranz, L. Cabrol, M. Carballa, A. Donoso-Bravo, L. Cruz, G. Ruiz-Filippi, R. Chamy, J.M. Lema, Relationship between phenol degradation efficiency and microbial community structure in an anaerobic SBR, Water Res. 47 (2013) 6739–6749. /10.1016/j.watres.2013.09.004.
[45] J. Gerritsen, S. Fuentes, W. Grievink, L. van Niftrik, B.J. Tindall, H.M. Timmerman, G.T. Rijkers, H. Smidt, Characterization of Romboutsia ilealis gen. nov., sp. nov., isolated from the gastro-intestinal tract of a rat, and proposal for the reclassification of five closely related members of the genus Clostridium into the genera Romboutsia gen. nov., Intestinib, Int. J. Syst. Evol. Microbiol. 64 (2014) 1600–1616. /10.1099/ijs.0.059543-0.
[46] W.H. Schwarz, The cellulosome and cellulose degradation by anaerobic bacteria, Appl. Microbiol. Biotechnol. 56 (2001) 634–649. /10.1007/s002530100710.
[47] J.H. Park, S.H. Lee, J.J. Yoon, S.H. Kim, H.D. Park, Predominance of cluster I Clostridium in hydrogen fermentation of galactose seeded with various heat-treated anaerobic sludges, Bioresour. Technol. 157 (2014) 98–106, https://doi.org/10.1016/j.biortech.2014.01.081.
[48] C.C. Wang, C.W. Chang, C.P. Chu, D.J. Lee, B.-V. Chang, C.S. Liao, Producing hydrogen from wastewater sludge by Clostridium bifermentans, J. Biotechnol. 102 (1) (2003) 83–92.
[49] A. Schnurer, B. Schink, B.H. Svensson, Clostridium ultunense sp. nov., a mesophilic bacterium oxidizing acetate in syntrophic association with a hydrogenotrophic methanogenic bacterium, Int. J. Syst. Bacteriol. 46 (4) (1996) 1145–1152.
[50] H. Xu, C. Wang, K. Yan, J. Wu, J. Zuo, K. Wang, Anaerobic granule-based biofilms formation reduces propionate accumulation under high H2 partial pressure using conductive carbon felt particles, Bioresour. Technol. 216 (2016) 677–683. /10.1016/j.biortech.2016.06.010.
[51] S. Kato, K. Hashimoto, K. Watanabe, Methanogenesis facilitated by electric syntrophy via (semi)conductive iron-oxide minerals, Environ. Microbiol. 14 (2012) 1646–1654, https://doi.org/10.1111/j.1462-2920.2011.02611.x.
[52] Q. Hu, D. Sun, Y. Ma, B. Qiu, Z. Guo, Conductive polyaniline nanorods enhanced methane production from anaerobic wastewater treatment, Polymer (Guildf). 120 (2017) 236–243. /10.1016/j.polymer.2017.05.073.
[53] L. Shao, S. Li, J. Cai, P. He, F. Lü, Ability of biochar to facilitate anaerobic digestion is restricted to stressed surroundings, J. Clean. Prod. 238 (2019) 117959. /10.1016/j.jclepro.2019.117959.
[54] A.J.M. Stams, K.C.F. Grolle, C.T.M. Frijters, J.B. Van Lier, Van Lier, Enrichment of thermophilic propionate-oxidizing bacteria in syntrophy with Methanobacterium thermoautotrophicum or Methanobacterium thermoformicicum, Appl. Environ. Microbiol. 58 (1) (1992) 346–352.
[55] A. Conklin, H.D. Stensel, J. Ferguson, Growth kinetics and competition between methanosarcina and methanosaeta in mesophilic anaerobic digestion, Water Environ. Res. 78 (5) (2006) 486–496.

[56] R. Rajagopal, D.I. Massé, G. Singh, A critical review on inhibition of anaerobic digestion process by excess ammonia, Bioresour. Technol. 143 (2013) 632–641, https://doi.org/10.1016/j.biortech.2013.06.030.
[57] F. Liu, A. Rotaru, P.M. Shrestha, N.S. Malvankar, K.P. Nevin, D.R. Lovley, Environmental Science Promoting direct interspecies electron transfer with activated carbon, Energy Environ. Sci. (2012) 8982–8989, https://doi.org/10.1039/c2ee22459c.
[58] R. Mei, M.K. Nobu, T. Narihiro, J. Yu, A. Sathyagal, E. Willman, W.T. Liu, Novel Geobacter species and diverse methanogens contribute to enhanced methane production in media-added methanogenic reactors, Water Res. 147 (2018) 403–412. /10.1016/j.watres.2018.10.026.
[59] M. Wang, Z. Zhao, Y. Zhang, Magnetite-contained biochar derived from fenton sludge modulated electron transfer of microorganisms in anaerobic digestion, J. Hazard. Mater. 403 (2021), 123972, https://doi.org/10.1016/j.jhazmat.2020.123972.
[60] Z. Wan, Y. Sun, D.C.W. Tsang, E. Khan, A.C.K. Yip, Y. Hau, Customised fabrication of nitrogen-doped biochar for environmental and energy applications, Chem. Eng. J. 401 (2020) 126136. /10.1016/j.cej.2020.126136.